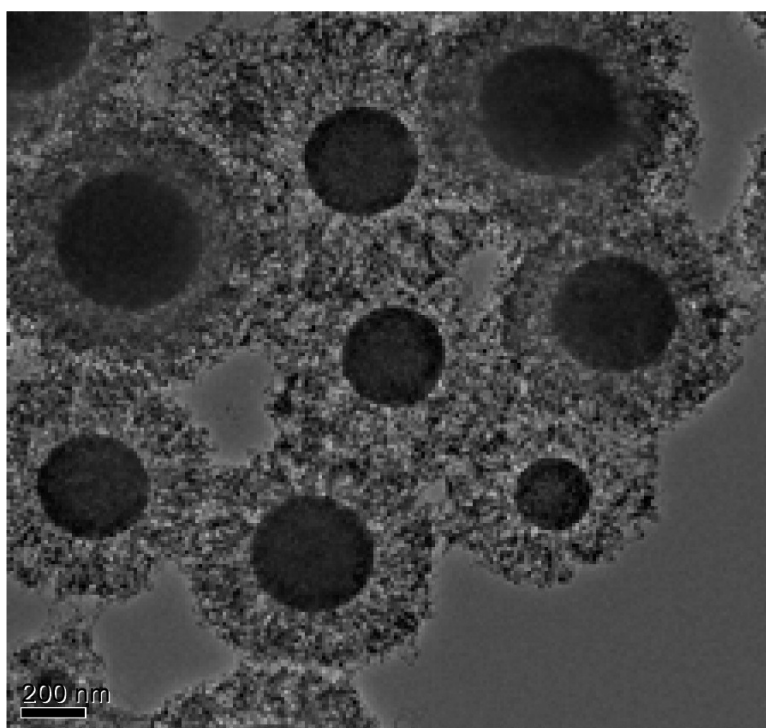


## Synthesis of Length-Controlled Aerosol Carbon Nanotubes and Their Dispersion Stability in Aqueous Solution

Young Kyun Moon, Jaebeom Lee, Jae Keun Lee, Tae Kyu Kim, and Soo H. Kim

*Langmuir*, 2009, 25 (3), 1739-1743 • DOI: 10.1021/la8031368 • Publication Date (Web): 08 January 2009

Downloaded from <http://pubs.acs.org> on February 13, 2009



### More About This Article

Additional resources and features associated with this article are available within the HTML version:

- Supporting Information
- Access to high resolution figures
- Links to articles and content related to this article
- Copyright permission to reproduce figures and/or text from this article



**ACS Publications**  
High quality. High impact.

# Langmuir

Subscriber access provided by PUSAN NAT UNIV CENTRAL LIB

[View the Full Text HTML](#)



**ACS Publications**  
High quality. High impact.

Langmuir is published by the American Chemical Society, 1155 Sixteenth Street N.W., Washington, DC 20036

# Synthesis of Length-Controlled Aerosol Carbon Nanotubes and Their Dispersion Stability in Aqueous Solution

Young Kyun Moon,<sup>†</sup> Jaebeom Lee,<sup>‡</sup> Jae Keun Lee,<sup>§</sup> Tae Kyu Kim,<sup>†</sup> and Soo H. Kim<sup>\*†</sup>

Department of Nanosystem and Nanoprocess Engineering, Pusan National University, 50 Cheonghak-ri, Samnangjin-eup, Mirayng-si, Gyeongnam 627-706, Korea, Department of NanoMedical Engineering, Pusan National University, 50 Cheonghak-ri, Samnangjin-eup, Mirayng-si, Gyeongnam 627-706, Korea, and School of Mechanical Engineering, Pusan National University, 30 Jangjeon-dong, Geumjeong-gu, Busan 609-735, Korea

Received September 24, 2008. Revised Manuscript Received December 8, 2008

A one-step method combining spray pyrolysis and thermal chemical vapor deposition (CVD) processes was developed to grow hybrid carbon nanotube (CNT)–bimetallic composite particles. Nickel, aluminum, and acetylene were used as the catalytic site, noncatalytic matrix, and hydrocarbon source, respectively. The bimetallic particles (i.e., Al–Ni) were spray pyrolyzed and subsequently passed through thermal CVD. During the thermal CVD, the catalytic decomposition of acetylene occurred on the free-floating bimetallic particles so that sea urchin-like CNTs were radially grown. Scanning electron microscopy (SEM) and transmission electron microscopy (TEM) analyses revealed the CNTs to have a uniform diameter of  $\sim 10 \pm 2$  nm. The length of the CNTs was controlled by varying the residence time of the bimetallic nanoparticles with a length of 200–1000 nm. After nitric acid treatment, the CNTs were released by melting the bimetallic particles. The resulting CNTs were then dispersed in an aqueous solution to examine the effect of the length of CNTs on their dispersion stability, which is a critical issue for the stability and repeatability of the heat transfer performance in nanofluids. Ultraviolet–visible (UV–vis) spectrometer analysis showed that shorter CNTs were less stable than the longer CNTs due to the higher mobility-induced agglomeration of the shorter CNTs.

## 1. Introduction

The gas-phase growth of carbon nanotubes (CNTs) provides the major advantage of continuous production of high purity CNTs. Various gas phase CNT production methods have been developed, including laser ablation,<sup>1</sup> wet chemistry,<sup>2</sup> and the HiPCO<sup>3</sup> processes. However, the CNTs grown using previous gas-phase methods were highly agglomerated at high production rates. In addition, they have very broad size and length distributions due to the continuous change in size and shape of the catalytic seed particles in the gas phase. Controlling the nanostructures of CNTs provides an innovative means of enhancing the mechanical, electrical, chemical, and thermal properties of CNT-based composite materials or devices.<sup>4–6</sup>

We and others have developed methods to control the diameter of gas phase-grown CNTs by controlling the size of the catalytic seed particles using either gas-phase electrophoretic tools<sup>7</sup> or wet chemistry-based metallic particles.<sup>8</sup> Both approaches produce size-controlled monodisperse particles, onto which CNTs are catalytically grown. However, they have inherent problems that

result in low production rates of CNTs and require expensive and complex auxiliary systems, particularly in the case of laser ablation.<sup>7</sup>

In this study, a one-step, simple and inexpensive method that enables the production of CNTs with relatively uniform diameter and controlled length grown on bimetallic aerosol nanoparticles was developed to overcome the difficulties in controlling the nanostructures of CNTs and increase the yield in the gas phase. The process involved a combination of spray pyrolysis and thermal chemical vapor deposition (CVD). Spray pyrolysis was used to produce bimetallic nanoparticles, which consisted of catalytic (i.e., guest nickel sites) and noncatalytic particles (i.e., host aluminum matrix). This process has the advantage of the versatile, economical, and continuous high purity production of metallic seed particles under a simple reactor design. After generating the free-floating bimetallic nanoparticles in the spray pyrolysis process, a subsequent thermal CVD process was carried out to grow the CNTs with controlled nanostructures by controlling the hydrocarbon source, reaction temperature, and residence time.

This approach has the potential advantages of providing less agglomerated CNTs in high yield by anchoring the bundles of CNTs to the surface of the bimetallic particles, and releasing the CNTs by acid etching into an aqueous solvent for the desired time and conditions. The latter was also investigated systematically as a potential application of this approach. Enhancing the dispersion of CNTs is a critical issue in the preparation of CNT-dispersed nanofluids. Various physical blending techniques<sup>9–11</sup> or chemical functionalization techniques<sup>12–14</sup> have been devel-

\* Corresponding author. Tel.: +82-55-350-5287. Fax: +82-55-350-5653. E-mail address: sookim@pusan.ac.kr.

<sup>†</sup> Department of Nanosystem and Nanoprocess Engineering.

<sup>‡</sup> Department of NanoMedical Engineering.

<sup>§</sup> School of Mechanical Engineering.

(1) Vander Wal, R. L.; Ticich, T. M.; Curtis, V. E. *J. Phys. Chem. B* **2000**, *104*(49), 11606.

(2) Sato, S.; Kawabata, A.; Nihei, M.; Awano, Y. *Chem. Phys. Lett.* **2003**, *382*, 361.

(3) Nikolaev, P.; Bronikowski, M. J.; Bradley, R. K.; Rohmund, F.; Colbert, D. T.; Smith, K. A.; Smalley, R. E. *Chem. Phys. Lett.* **1999**, *313*, 91.

(4) Subramoney, S.; Ruoff, R. S.; Lorents, D. C.; Malhotra, R. *Nature* **1993**, *366*, 637.

(5) Yang, C.; Wang, D.; Hu, X.; Dai, C.; Zhang, L. *J. Alloys Compd.* **2008**, *448*, 109.

(6) Ruoff, R. S.; Lorents, D. C. *Carbon* **1995**, *33*(7), 925.

(7) Kim, S. H.; Zachariah, M. R. *Mater. Lett.* **2007**, *61*, 2079.

(8) Cheung, C. L.; Kurtz, A.; Park, H.; Lieber, C. M. *J. Phys. Chem. B* **2002**, *106*(10), 2429.

(9) Wasan, D.; Nikolov, A.; Moudgil, B. *Powder Technol.* **2005**, *153*, 135.

(10) Yoshida, H.; Nurtono, T.; Fukui, K. *Powder Technol.* **2005**, *150*, 9.

(11) Hwang, Y.; Lee, J. K.; Lee, J. K.; Jeong, Y. M.; Cheong, S. I.; Ahn, Y. C.; Kim, S. H. *Powder Technol.* **2008**, *186*(2), 145.

(12) Jiang, L.; Gao, L.; Sun, J. *J. Colloid Interface Sci.* **2003**, *260*(1), 89.

(13) Xie, H.; Lee, H.; Youn, W.; Choi, M. *J. Appl. Phys.* **2003**, *94*, 4967.

(14) Kim, D. H.; Hwang, Y. J.; Cheong, S. I.; Lee, J. K.; Hong, D. S.; Moon, S. Y.; Lee, J. E.; Kim, S. H. *J. Nanopart. Res.* **2008**, *10*, 1121.

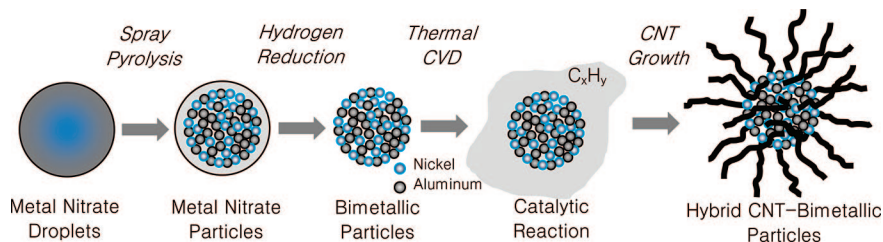


**Figure 1.** Schematic of the growth mechanism of aerosol CNTs–bimetallic composite particles.

oped to homogeneously disperse CNTs in deionized water or various organic solvents. Although there are no universal methods, UV–vis spectroscopy has been used to determine the concentration and dispersion stability of CNTs in a variety of solvents.<sup>15</sup> However, the optical absorbance of CNTs is strongly affected by many parameters, such as the diameter, length, and concentration of the CNTs as well as the degree of agglomeration. Therefore, the second aim of this study was to systematically examine the effect of CNT nanostructures with a uniform diameter and controlled length on the dispersion stability in an aqueous solution.

## 2. Experiment

### 2.1. Synthesis of Hybrid CNT–Bimetallic Composite Particles.

The gas-phase growth of aerosol CNTs was carried out using a combination of spray pyrolysis and thermal CVD processes. Briefly, the first step involved the preparation of a precursor solution, which was composed of aluminum nitrate nonahydrate ( $\text{Al}(\text{NO}_3)_3 \cdot 9\text{H}_2\text{O}$ , Sigma Aldrich)/nickel nitrate hexahydrate ( $\text{Ni}(\text{NO}_3)_2 \cdot 6\text{H}_2\text{O}$ , Sigma Aldrich) at a 1:1 molar ratio in deionized water (> 18 Mohm) with a total concentration of ~3 wt %. The mixed metal nitrate precursor solution was aerosolized using an ultrasonic nebulizer, where a controlled amount of nitrogen gas (< ~5 lpm) was supplied to rapidly transport the aerosolized metal nitrate droplets. After passing through a subsequent silica-gel-assisted drying process, the resulting particles were mixed with hydrogen gas at a flow rate of ~100 sccm in the first electric tube furnace heated to ~1000 °C to decompose the metal nitrate nanoparticles into pure bimetallic nanoparticles. The tube furnace had a heating length of ~30 cm and a quartz tube diameter of ~2.54 cm. These spray pyrolyzed bimetallic nanoparticles were then introduced into the second tube furnace, where they were mixed with acetylene ( $\text{C}_2\text{H}_2$ ) gas at a flow rate of ~15 sccm and heated simultaneously at ~750 °C to catalytically grow the CNTs on the surface of the bimetallic aerosol nanoparticles. Here, the second tube furnace was set up vertically because it can minimize the thermophoretic loss of the final products from the thermal CVD process. The residence time of bimetallic nanoparticles in the thermal CVD reactor was varied from 10 to 90 s by controlling the flow rate of nitrogen carrier gas from 5 down to 0.5 lpm, respectively. The resulting hybrid CNT–bimetallic composite particles were collected on a membrane filter with a pore size of ~200 nm.

**2.2. Preparation and Characterization of CNT-Dispersed Aqueous Nanofluids.** To prepare a homogeneous suspension of the CNTs released in a surfactant-free aqueous solution, 30 mg of CNT–bimetallic composite particles were heated under reflux for 1 h in 40 mL of nitric acid. The resulting mixture was then filtered and washed to remove any residual acidity. The resulting CNTs collected on the membrane filter were dried at ~100 °C for 4 h. And then an ultrasonic bath operated at a frequency of 40 kHz and a power of 200 W was employed to sonicate surface-modified CNTs in deionized water for 2 h. A nitric acid treatment induces chemical oxidation of carbon materials, which forms a hydrophilic surface structure on the carbon materials.<sup>16</sup> The morphology of the resulting

materials was characterized by a scanning electron microscope (SEM; Hitachi, Ltd., model S-4200), which was operated at ~15 kV, and a transmission electron microscope (TEM; JEOL Corporation, model JEM 2011), which was operated at ~100 kV. The optical absorbance of the CNTs was measured using an ultraviolet–visible (UV–vis) spectrometer (Scinco, model S-3100). A Zetasizer (Malvern, model ZEN 3500) was used to observe the dispersion state (i.e., zeta potential) and the relative hydrodynamic diameter distribution of the CNT aqueous suspension. In addition, a pH meter (Mettler Toledo, model 7 Multi TM) was used to measure the pH of various CNT-dispersed aqueous solutions.

## 3. Results and Discussion

Figure 1 shows the possible growth mechanism of the hybrid CNT–bimetallic composite particles. Atomizing the precursor solution produces discrete aerosol droplets, containing two metallic nitrates (i.e., nickel nitrate and aluminum nitrate). In the evaporating droplets, the solute concentration reaches a supersaturated state and metal nitrate sites begin to nucleate on the surface of the aerosol droplets. Subsequently, these metal nitrate particles are mixed with hydrogen gas and heated to ~1000 °C in the first tube furnace to form pure bimetallic particles containing both catalytic nickel sites and a noncatalytic aluminum matrix. The addition of acetylene gas to the pure bimetallic particles in the second tube furnace heated at 750 °C promotes the formation of CNTs on the surface of the bimetallic particles (see Figure 2). Reactions at temperatures >750 °C result in the direct decomposition of acetylene, and then make the coating of the bimetallic particles with carbon, which inhibits the growth of CNTs.<sup>17</sup>

It is believed that the residence time ( $t_r$ ) of the reacting bimetallic particles within thermal CVD reactor is the key for CNT growth on the nickel sites in the aluminum matrix resulting from catalytic decomposition of acetylene. The SEM images of CNTs in Figure 2 show hairy CNTs grown homogeneously over the entire surface of spherical bimetallic particles. This suggests indirectly that the catalytic nickel sites are distributed homogeneously in the noncatalytic aluminum matrix.<sup>18–21</sup> As the residence time of the bimetallic particles was reduced in the thermal CVD reactor, the length of the CNTs was clearly observed to become shorter. It should be noted that the maximum production rate of CNT–bimetallic composite particles was ~13  $\text{mg} \cdot \text{h}^{-1}$ , which is much higher than that of the pulsed laser ablation (PLA) system-assisted CNT–nickel nanoparticle generation method (i.e., ~1.3  $\text{mg} \cdot \text{h}^{-1}$ ).<sup>7</sup> In order to compare the mass production rates of pure CNTs formed, metal particles were removed from the CNT–metallic composite particles via acid treatment, which will be discussed

(17) Kim, S. H.; Zachariah, M. R. *J. Phys. Chem. B* **2006**, *110*, 4555.

(18) Iida, N.; Naito, H.; Ito, H.; Nakayama, K.; Lenggono, I. W.; Okuyama, K. *J. Ceram. Soc. Japan* **2004**, *112*(1307), 405–408.

(19) Strobel, R.; Grunwaldt, J.-D.; Camenzind, A.; Pratsinis, S. E.; Baiker, A. *Catal. Lett.* **2005**, *104*(1–2), 9–16.

(20) Azurdia, J. A.; Marchal, J.; Shea, P.; Sun, H.; Pan, X. Q.; Laine, R. M. *Chem. Mater.* **2006**, *18*(3), 731–739.

(21) Pingali, K. C.; Deng, S.; Rockstraw, D. A. *Powder Technol.* **2008**, *187*(1), 19–26.

(15) Li, Z. F.; Luo, G. H.; Zhou, W. P.; Wei, F.; Xiang, R.; Liu, Y. P. *Nanotechnology* **2006**, *17*, 3692.

(16) Esumi, K.; Ishigami, M.; Nakajima, A.; Sawada, K.; Honda, H. *Carbon* **1996**, *34*(2), 279.



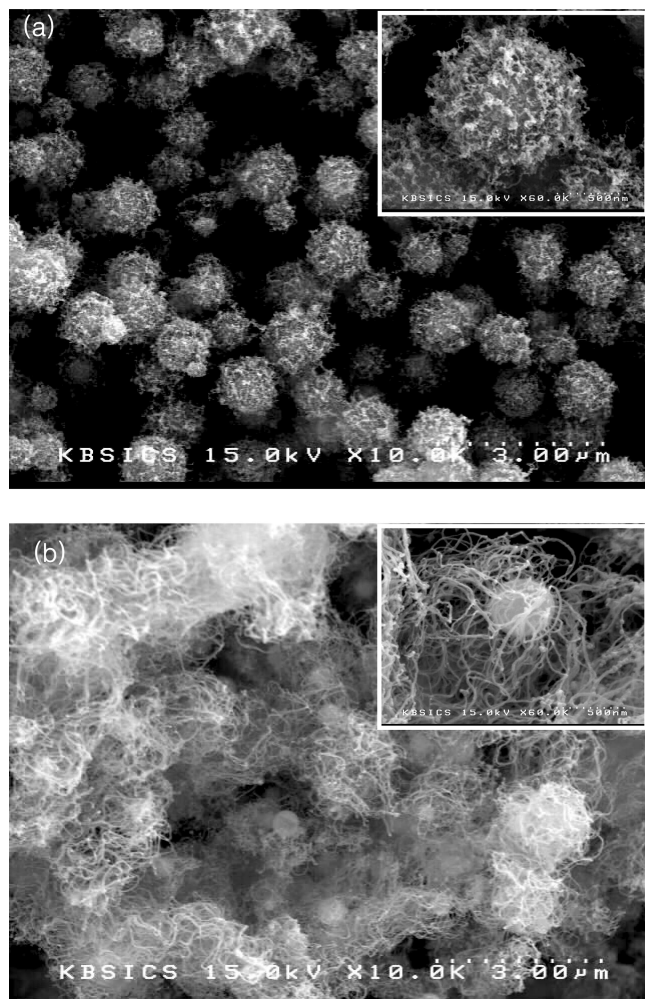


**Figure 2.** Low-resolution SEM images of the hybrid Ni/Al/CNT composite particles grown by thermal CVD at a reaction time of (a)  $\sim 10$  s and (b)  $\sim 50$  s. (The insets are high-resolution SEM images.)

later in detail. The conversion rate of carbon from acetylene to CNTs in this approach was then calculated to be  $\sim 1.8\%$  based on the ratio of the mass production rate of pure CNTs of  $\sim 8 \text{ mg} \cdot \text{h}^{-1}$  to the mass supplying rate of the carbon source of  $\sim 445 \text{ mg} \cdot \text{h}^{-1}$  (i.e.,  $\text{C}_2\text{H}_2$  flow rate of  $\sim 15 \text{ sccm}$ ). In the same manner, the conversion rate of carbon in the PLA-assisted method<sup>7</sup> was calculated approximately to be  $\sim 0.34\%$  based on the ratio of the mass production rate of pure CNTs of  $\sim 0.5 \text{ mg} \cdot \text{h}^{-1}$  to the mass supplying rate of the carbon source of  $\sim 148 \text{ mg} \cdot \text{h}^{-1}$  (i.e.,  $\text{C}_2\text{H}_2$  flow rate of  $\sim 5 \text{ sccm}$ ).<sup>7</sup> This indicates that the yield of CNTs formed by the combination of spray pyrolysis and thermal CVD in this approach is approximately 5 times higher than that of CNTs formed by the PLA-assisted method.

With the corroboration of the TEM analysis as shown in Figure 3, bimetallic particles with an average diameter of  $\sim 300 \text{ nm}$  were observed to have CNTs with average lengths of  $200 \pm 40 \text{ nm}$  (Figure 3a) at  $t_r = \sim 10 \text{ s}$  and  $1000 \pm 200 \text{ nm}$  (Figure 3b) at  $t_r = \sim 50 \text{ s}$ , respectively. High-resolution TEM (HRTEM) analysis of the CNTs grown on bimetallic aerosol nanoparticles in Figure 3c,d indicates that multiwall CNTs with relatively uniform diameters of  $\sim 10 \pm 2 \text{ nm}$  were immobilized by sticking on the surface of bimetallic particles. Also the CNTs grown are inherently bent and composed of up to  $\sim 15$  walls and a hollow core. The growth rate of the aerosol CNTs in this approach was calculated to be approximately  $\sim 20 \text{ nm} \cdot \text{s}^{-1}$ , which appears to be much smaller than the theoretically calculated growth rate for

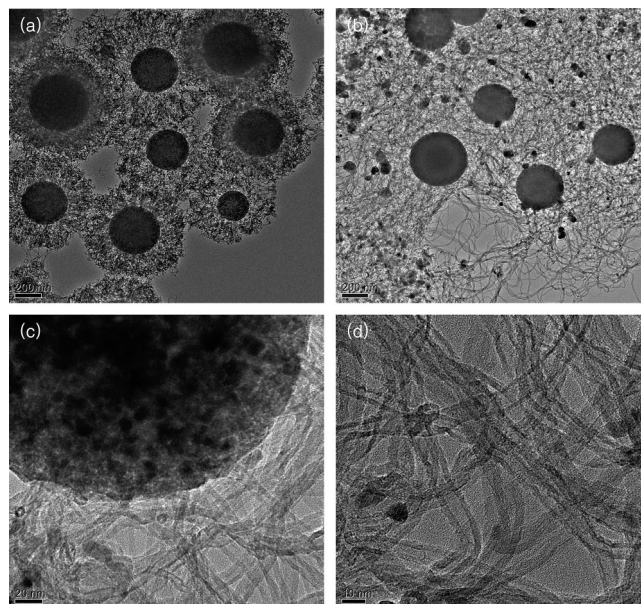


**Figure 3.** TEM images of the Ni/Al/CNT composite particles grown by thermal CVD for a reaction time of (a)  $\sim 10 \text{ s}$  and (b)  $\sim 50 \text{ s}$ . HRTEM images of (c) the interface between the metallic particle surface and CNTs and (d) multiwalled CNTs with relatively uniform diameters.

CNTs of  $\sim 70 \text{ nm} \cdot \text{s}^{-1}$  with a carbon diffusivity of  $\sim 1.94 \times 10^{-9} \text{ cm}^2 \cdot \text{s}^{-1}$  and a carbon solubility of  $\sim 7.05 \times 10^{-3} \text{ g} \cdot \text{cm}^{-3}$  in nickel particles of  $\sim 10 \text{ nm}$  in diameter.<sup>22</sup> The discrepancy between the experimentally and theoretically determined growth rates of CNTs was attributed to the nickel sites in the bimetallic particles being poisoned by the presence of the aluminum matrix, which appeared to significantly decrease the carbon solubility in nickel. As the residence time was further decreased to much less than  $\sim 10 \text{ s}$ , the nonhomogeneous growth of CNTs was observed on the surface of bimetallic particles, suggesting that amorphous carbon or CNT nuclei were formed irregularly due to the insufficient catalytic reaction time between the bimetallic particles and hydrocarbon gas in such a short residence time. Therefore, critical residence time of the catalytic particles in the thermal CVD reactor is required to ensure the homogeneous formation of a large population of CNTs. It should be also noted that there was no appreciable change in the average length of CNTs with  $\sim 1000 \pm 200 \text{ nm}$  at longer than the residence time of  $\sim 50 \text{ s}$ , indicating that catalytic sites of nickel on the surface of bimetallic particles were deactivated by coking.

One potential advantage of controlling the length of CNTs using this approach is that it enables an examination of the effect of length on the behavior of CNTs in a liquid medium. In order to vary the length of CNTs, many researchers have used ultrasonication to cut the relatively long CNTs into shorter CNTs.<sup>23</sup> However, varying the ultrasonication treatment time for long CNTs simply results in the formation of shorter CNTs with an ill-defined broad length distribution, which can mask the essential length effect of the CNTs on their thermal, physical, or chemical behavior in the liquid medium. In order to examine the behavior of pure CNTs in a liquid medium in this approach, the metallic particle root first needs to be removed by a nitric acid treatment for 1 h at  $\sim 100 \text{ }^\circ\text{C}$ . Figure 4a,c shows SEM images of the short CNTs (hereafter S-CNTs, which have an aspect ratio of  $\sim 20$ ) and long CNTs (hereafter L-CNTs, which

(22) Lander, J. J.; Kern, H. E.; Beach, A. L. *J. Appl. Phys.* **1952**, 23(12), 1305.

(23) Glory, J.; Bonetti, M.; Helezen, M.; Mayne-L'Hermite, M.; Reynaud, C. *J. Appl. Phys.* **2008**, 103(9), 094309.

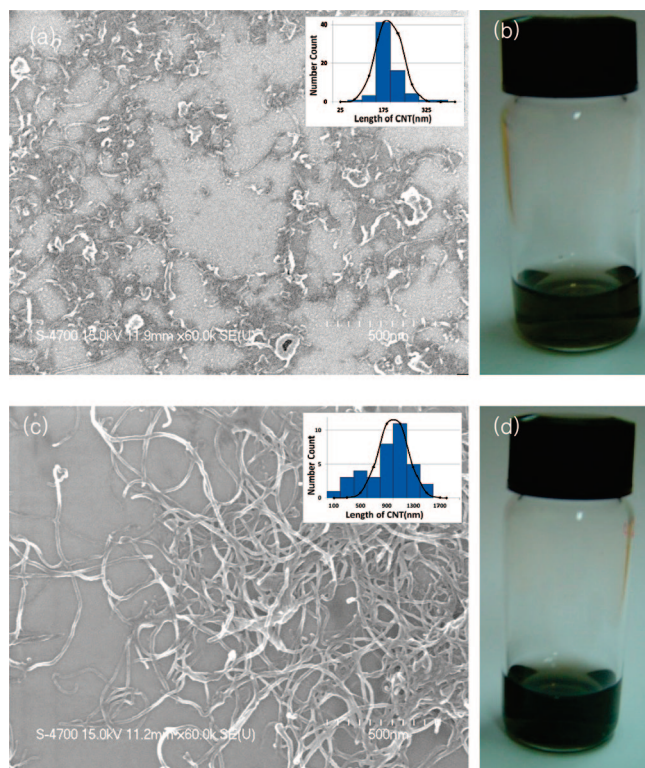


**Figure 4.** SEM images of (a) S-CNTs (i.e., aspect ratio =  $\sim 20$ ) and (c) L-CNTs (i.e., aspect ratio =  $\sim 100$ ) released by the nitric acid treatment and dispersed on the surface of the silicon substrate, and images of vials containing (b) S-CNT- and (d) L-CNT-dispersed aqueous nanofluids after 2 weeks had passed from the initial preparation (experimental conditions: CNT concentration = 0.001 wt % for both L-CNTs and S-CNTs; zeta potential =  $-50.23$  mV and pH = 7.02 for L-CNTs; and zeta potential =  $-43.67$  mV and pH = 6.94 for S-CNTs).

have an aspect ratio of  $\sim 100$ ) released from the bimetallic particles after the nitric acid treatment. This nitric acid treatment also changes the hydrophobic surface of the CNTs into a hydrophilic surface, which eventually helps the CNTs with a homogeneous dispersion in deionized water. Relatively high zeta potentials of  $-50.23$  mV for the L-CNTs aqueous nanofluid and  $-43.67$  mV for the S-CNTs aqueous nanofluid were also measured at a pH value of  $\sim 7$ . The CNT-dispersed aqueous solutions prepared at a concentration of  $\sim 0.010$  mg $\cdot$ ml $^{-1}$  did not show any visible precipitates in the vials even after 2 weeks, as shown in Figure 4b,d. On the basis of results of zeta potential measurements, we assumed that both S-CNTs and L-CNTs have very similar hydrophilic properties via nitric acid treatment and homogeneous distribution in the aqueous solutions via strong ultrasonication, such that the Brownian movement of the CNTs plays the key role of disturbing the dispersion state of the CNTs in the aqueous solutions.

After the controlled release of CNTs via a nitric acid treatment, the two groups of CNTs, L-CNTs and S-CNTs, were dispersed in deionized water. Dynamic light scattering (DLS, i.e., a Zetasizer) was first used to estimate the relative particle size distribution of the L-CNTs and S-CNTs dispersed in deionized water. The measured particle size distribution using the DLS system does not correspond to the real nanostructures of the CNTs because the CNTs have a high aspect ratio and absorptive property. However, the evolution of relative particle size distributions, corresponding to each group of CNTs with different lengths, could be observed as a function of the elapsed time. Figure 5a,b shows that the average hydrodynamic diameters of S-CNTs and L-CNTs increased slightly with increasing elapsed

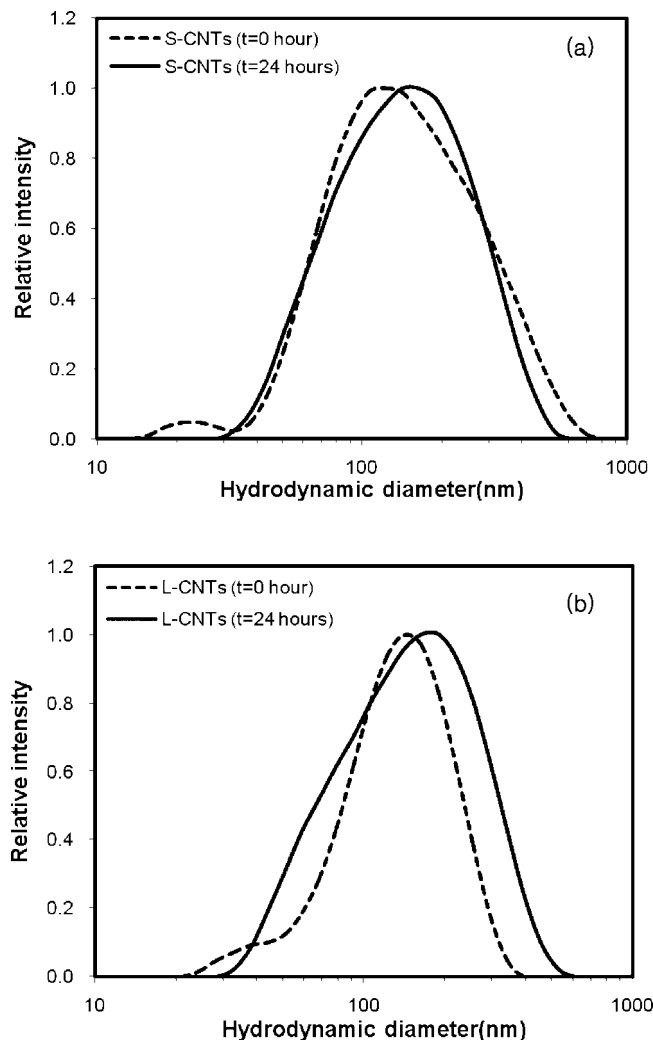


**Figure 5.** Hydrodynamic diameter distributions of (a) S-CNTs and (b) L-CNTs in deionized water measured by DLS at an elapsed time of  $t = 0$  h (i.e., initial preparation of CNT-based solution) and 24 h after sonication.

time. The initial diffusion coefficients of  $4.16$   $\mu\text{m}^2\cdot\text{s}^{-1}$  for S-CNTs and  $3.87$   $\mu\text{m}^2\cdot\text{s}^{-1}$  for L-CNTs were also found to decrease to a value of  $3.96$   $\mu\text{m}^2\cdot\text{s}^{-1}$  for S-CNTs and  $3.80$   $\mu\text{m}^2\cdot\text{s}^{-1}$  for L-CNTs in 24 h. This indicates that the CNTs began to agglomerate to some extent in the deionized water, and S-CNTs especially seem to make agglomeration faster than L-CNTs due to the higher mobility of S-CNTs.

UV-vis spectroscopy was carried out to quantify the dispersion stability of CNTs. First, the absorbance at the wavelength of 500 nm was plotted as a function of the concentration of CNTs for both the L-CNT- and S-CNT-dispersed aqueous nanofluids. According to the Beer-Lambert law (i.e.,  $A = \epsilon Lc$ , where  $\epsilon$  is the absorption coefficient,  $L$  is the distance that light beam travels through the colloidal solution ( $= 1$  cm), and  $c$  is the CNT concentration), the slopes of the absorbance vs CNT concentration lines are the absorption coefficients,<sup>15</sup> which were found to be  $\sim 42.58$  mL $\cdot$ mg $^{-1}\cdot$ cm $^{-1}$  for L-CNTs and  $\sim 34.88$  mL $\cdot$ mg $^{-1}\cdot$ cm $^{-1}$  for S-CNTs as shown in Figure 6a. The variation in these adsorption coefficients was due to an experimental error of  $\pm 15\%$ . These absorption coefficients were quite similar to the  $42.20$  mL $\cdot$ mg $^{-1}\cdot$ cm $^{-1}$  and  $39.92$  mL $\cdot$ mg $^{-1}\cdot$ cm $^{-1}$  reported elsewhere, where MWCNTs were dispersed either in chloroform



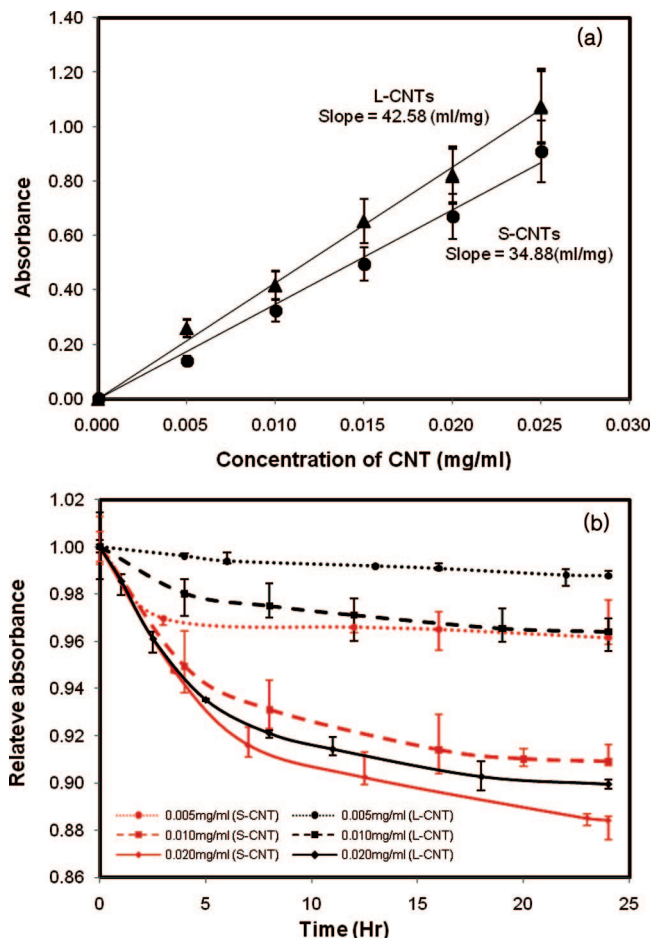


**Figure 6.** (a) Absorbance of the L-CNTs and S-CNTs at a wavelength of 500 nm as a function of the concentration of CNTs. (b) Relative absorbance of the L-CNTs and S-CNTs as a function of the elapsed time and concentration.

in the presence of polybutadiene<sup>24</sup> or in deionized water by ultrasonication.<sup>15</sup> This suggests that the absorption coefficients of CNTs are a weak function of the aspect ratio of CNTs.

In order to confirm the effect of CNT length on their dispersion stability, two groups of L-CNT- and S-CNT-dispersed aqueous solutions were prepared with three different concentrations of 0.005, 0.010, and 0.020 mg·ml<sup>-1</sup>. The absorbance at a given time was integrated at the wavelength range of 700–1000 nm, in which there was no appreciable change in absorbance as a function of wavelength. This suggests that the major factor

influencing the absorbance is the dispersion state of CNTs in aqueous solutions. The dispersion stability of CNTs in the aqueous solution was evaluated by calculating the relative absorbance with the ratio of the integrated absorbance of CNTs at the initial time to the integrated absorbance of CNTs at each elapsed time. The relative absorbance of each CNT-dispersed aqueous solution group (i.e., L-CNTs and S-CNTs) was measured by UV–vis spectroscopy for ~24 h, as shown in Figure 6b. It should be noted that the S-CNTs had a much lower relative absorbance than the L-CNTs for all three different concentrations. This suggests that S-CNTs have relatively lower long-term dispersion stability because they tend to have a higher degree of agglomeration with elapsed time on account of their higher mobility relative to that of L-CNTs.

#### 4. Conclusions

This paper reports a method for producing length-controlled CNTs with sea urchin-like shapes, which were grown on bimetallic aerosol nanoparticles in the gas phase. In this approach, a combination of conventional spray pyrolysis and thermal CVD processes enables the formation of CNTs with uniform diameters of  $\sim 10 \pm 2$  nm, a controlled-length of 200–1000 nm, and a maximum production rate of  $\sim 13$  mg·h<sup>-1</sup>. The gas-phase growth of CNTs occurred on the nickel sites in the aluminum matrix, which were presented within the bimetallic nanoparticle form. The length of the CNTs was controlled by varying the residence time of the reacting bimetallic nanoparticles during the thermal CVD process. After producing the length-controlled CNTs, they were released by a nitric acid treatment, and the effect of their length on the dispersion stability in aqueous nanofluids was examined. Shorter CNTs had lower dispersion stability, presumably due to the higher mobility-induced agglomeration in the aqueous solution. The potential advantages of this approach are that (i) it produces a high volume of unagglomerated CNTs with controlled nanostructures and high purity under a relatively short residence time of less than  $\sim 50$  s, and (ii) the CNTs can be released by a nitric acid treatment at a desired time and conditions. This can allow an examination of the effect of the aspect ratio of CNTs on their mechanical, electrical, and thermal properties in a given medium (e.g., polymer, organic or inorganic solvent, etc.).

**Acknowledgment.** This study was supported by a Korean Science and Engineering Foundation (KOSEF) grant funded by the Korean government (MEST) (No. R01-2008-000-10181-0).

**Supporting Information Available:** Raman spectra of short and long sea urchin-like CNTs before and after acid treatment. This material is available free of charge via the Internet at <http://pubs.acs.org>.

(24) Baskaran, D.; Mays, J. W.; Bratcher, M. S. *Chem. Mater.* **2005**, *17*(13), 3389.